A Potent Peroxidase from Solid Cell Culture of *Ocimum Basilicum* with High Sensitivity for Blood Glucose Determination

Parvin Mohammadnejad
National Institute for Genetic Engineering and Biotechnology
Saeed Soleimani Asl
National Institute for Genetic Engineering and Biotechnology
Zahra Rasoulian
National Institute for Genetic Engineering and Biotechnology
Saeed Aminzadeh
National Institute for Genetic Engineering and Biotechnology
Jaleh Ghashghaie
Paris-Sud University: Universite Paris-Saclay
Kamahldin Haghbeen (kamahl@nigeb.ac.ir)
National Institute for Genetic Engineering and Biotechnology https://orcid.org/0000-0003-3011-5629

Research Article

Keywords: Antioxidant, Basil, Diazo compound, Joint-enzymatic assay

Posted Date: February 23rd, 2021

DOI: https://doi.org/10.21203/rs.3.rs-227761/v1

Version of Record: A version of this preprint was published at Plant Cell, Tissue and Organ Culture (PCTOC) on April 8th, 2021. See the published version at https://doi.org/10.1007/s11240-021-02076-5.

Abstract

Extensive applications of peroxidase (POX) have raised the global market demand at a considerable rate during the forecast period of 2020 - 2025. Nonetheless, the large-scale POX preparation still relies on the extraction from agricultural products, while there is an accumulative driving force toward employing biotechnological processes with agricultural hassle free identity. In pursuit of this trend, a novel heme peroxidase was purified to homogeneity (MW of 40 kD) from the callus culture of *Ocimum basilicum* L. in darkness on Murashige-Skoog medium supplemented by 2,4-dichlorophenoxyacetic acid (10^{-6} M) and kinetin (10^{-5} M). The highest activity of the purified peroxidase (ObPOX) was observed in Tris-base buffer at pH 7.5 and 80 °C. ObPOX showed high stability over pH(s) 5 to 7.5 and temperatures of 15 to 60 °C. ObPOX specific activity was 1245.142 AU mg^{-1} in the presence of phenol, 4 times higher than that of HRP. ObPOX showed moderate affinity for guaiacol (K_m = 21.5 mM), but obtained an exceptionally high specificity constant (k_{cat}/K_m = 66743.7 $s^{-1}M^{-1}$) for GASA (4-[(4-Hydroxy-3-methoxyphenyl) azo]-benzenesulfonic acid), the introduced substrate for determination of blood sugar. Applying ObPOX instead of HRP in glucose measurements of the real samples improved the regression constant of the correlation diagram between the tests and the lab results from 0.958 to 0.981. Physicochemical properties of ObPOX as well as the growth rate of basil callus (5.04 g L^{-1} per day) and the yield of ObPOX production (35 mg per 100 g dry biomass per subculture) designates *O. basilicum* cell culture for large-scale production of a robust peroxidase.

Introduction

Peroxidase (POX), EC number 1.11. 1. X, is a ubiquitous enzyme with numerous applications in nature and industries. About 80% of the discovered POXs belong to heme-peroxidases, which are categorized in two large families of peroxidase-cyclooxygenase (found in animals) and peroxidase-catalase (found in non-animal species) (Shigeto and Tsutsumi 2016). Established uses of POX in food, cosmetic, and health care industries as well as proven applicability in fabrication of biosensors, agricultural waste valorization, bio-bleaching and water and soil bioremediation have raised the global market demand at a considerable rate during the forecast period between 2020 and 2025 (Market Reports World. Horseradish Peroxidase (HRP) Market Size, Share 2020 Analysis, Revenue, Price, Market Share, Growth Rate, Forecast by 2024| Says Market Reports World. 2020). Nonetheless the large scale preparation of POX still relies on the extraction from agricultural products (González-Rábade et al. 2012), while there has been a remarkable shift toward employing biotechnological processes as well. The advantages of new technologies along with the increases in the costs of labor and energy accompanied by the shortages in agricultural land and water have speeded up this rather new trend (González-Rábade et al. 2012). Among the developed biotechnological techniques, plant cell and tissue culture has received special attention due to its uncomplicated setup prerequisites and high potential for production of numerous simple and complex natural molecules including enzymes (Fehér 2019; Rani and Abraham 2016). Because of totipotency of plant cells, this technology allows production of the desired molecules in either wild or genetically-modified cells, tissues, and the whole plant. However, each of these methods has its own advantages and

limitations. For instance, a techno-economic analysis study has shown that the transformed *Nicotiana benthamiana* can be used for production of horseradish peroxidase (HRP) in a biofarm platform with the proven plant yield of 240 mg HRP kg^{-1} biomass (Walwyn et al. 2015). In addition to the economically accepted yield, production of a single isozyme (HRP C) is the best advantage of this method. But this technology is still dependent on the agricultural provisions whereas plant cell and hairy root culture are bioreactor-based technologies, which make them free of the cultivation hassle (Ochoa-Villarreal et al. 2016). Plant cell culture can be carried out on jellified (solid) and in liquid (suspension) mediums. However, due to the problems associated with the latter one such as shear stress, foam formation, cells aggregation, and incompetent respiration and gas transport (Valdiani et al. 2019), there is an inclination toward using solid cell cultures as well as hairy root cultures (Efferth 2019; González-Rábade et al. 2012). There are reports that show the biomass growth, production of the desired compound, or both are heavily affected because of the shear stress of the suspension culture bioreactors (Haida et al. 2019), while solid cell culture is practically easier and economically more amenable (Efferth 2019; Ochoa-Villarreal et al. 2016). In view of these premises and in pursuit of a reliable source for a potent plant POX, solid culture of basil cells was thoroughly studied. Sweet basil (*Ocimum basilicum* L.) is a culinary and ornamental herb with high antioxidant capacity (Vlase et al. 2014). It has been recently shown that the solid cell culture of basil can be used for high-yield production of phenolic acids and anthocyanins by applying proper light cycles (Nazir et al. 2019). Recently, it has also been shown that blood sugar can be determined precisely in less than 30 seconds by using a diazo substrate for HRP vis the joint enzymatic reactions of glucose oxidase and a peroxidase (Mohammadnejad et al. 2020). In this work we demonstrate better performance of *Ocimum basilicum* peroxidase (ObPOX) as compared with that of HRP.

Materials And Methods

Chemicals and plant materials

HRP (C), phenylmethylsulfonyl fluoride (PMSF), hydrogen peroxide (H_2O_2), Folin-Ciocalteu reagent, phenol and ammonium sulfate were purchased from Merck (Darmstadt, Germany). 4-Aminoantipyrine (4AAP), 2,4-dichlorophenoxyacetic acid (2,4-D), N-(2-furanylmethyl)-1H-purin-6-amine (kinetin) and tetramethylethylenediamine (TEMED) were purchased from Sigma™ Chemical and Biochemical Company (St. Louis, MO, USA). Guaiacol was from Fluka Chemie GmbH. Catalase (CAT) was purchased from Serva electrophoresis GmbH (D-69115 Heidelberg). The azo dye 4-[(4-Hydroxy-3-methoxyphenyl) azo]-benzene sulfonic acid (GASA) was synthesized as described before (Haghbeen and Tan 1998). Sephadex G-50 and anionic diethylaminoethyl cellulose (DEAE-C) were purchased from Pharmacia. Seeds of *Ocimum basilicum* L. (Basil) were purchased from Pakan Bazr Company (http://www.pakanbazr.com). Other chemicals were taken from the authentic samples. Solid Murashige and Skoog medium (MS) was prepared according to the literature using 8 g L^{-1} of agar (Saad and Elshahed 2012). Spectrophotometric measurements were carried out using a UV/Visible Specord 50+ spectrophotometer (Analytik Jena, Germany). The results were analyzed using the Microsoft Office Excel.

Seed Germination and Callus Induction

The viable sterilized seeds sprouted on hormone-free MS supplemented with sucrose (3%) at pH 5.8. Seedlings were allowed to grow on the same medium in a growth chamber (25 ± 2 ºC, light/dark cycle of 16/8 h). To induce callus, the excised explants from the leaves of the young plantlets were put on a solid MS medium supplemented with sucrose (3.0%), 2,4-D (10^{-6} M) and kinetin (10^{-5}M) at the same pH and temperature. The resulting callus cells were proliferated on the same medium in the dark. The fast growing friable cells were selected and subcultured every 5 weeks. To calculate the biomass, the weights of the callus were recorded before and after drying at 37 °C for 48 h.

Callus extraction for total phenolic compounds (TPC) and radical scavenging activity (RSA) measurements

The desired fresh callus (2.5 g) was smashed and grounded in a mortar containing 5.0 to 10 mL of methanol (MeOH) or acetate buffer (0.02 M, pH 5.5). The resulting extract was centrifuged (1500 g, 15 min) using a Beckman Centrifuge, J-21 model, then filtered (Whatman® Ashless, Grade 42 Filtration Paper, Sigma) and maintained in the dark at 4.0 °C. TPC and RSA measurements were conducted according to the reported procedures (Khosravi et al. 2019).

Extraction and purification of ObPOX

Fresh *O. basilicum* callus (100 g) was homogenized in 200 mL of Tris-base buffer (0.01 M, pH 6.0) containing PMSF (0.55 µM) at 4.0 °C. The tissue debris was removed by centrifugation (8,000 g, 20 min at 4.0 °C). The pellet was washed twice using 20 mL of the extraction buffer, then it was added to the extract. The resulting homogenate crude extract was subjected to step-wise ammonium sulfate precipitation (20-80%). Based on the activity assay results, the sediment at 80% saturation was collected by centrifugation (12,000 g, 20 min, at 4.0 °C). Then, it was dissolved in a minimum volume of the extraction buffer for further experiments.

The solution of the previous step (1 mL) was chromatographed on a Sephadex G-50 column (2 × 50 cm) using Tris-base buffer (0.01 M, pH 6.0) as the mobile phase. The output of the column was monitored spectrophotometrically at λ = 280 nm. The collected fractions were checked for the POX activity at 516 nm as explained below. Based on the resulting chromatogram, the selected active fractions were pooled and loaded onto on a DEAE-C column (1×30 cm) equilibrated with Tris-base buffer (0.01 M, pH 6.0). Proteins were eluted with a stepwise gradient of 0.0–0.2 M NaCl in the same buffer. The fractions (1 mL) were examined at 280 nm. According to the resulting chromatogram, the selected active fractions were pooled and used in further experiments.

SDS-PAGE and two-dimensional electrophoresis

Protein content of the desired solutions was measured by Bradford method (Kruger 2009). SDS-PAGE of the samples was performed according to the standard Laemmli (Laemmli 1970). The protein bands were visualized by both Coomassie brilliant blue G250 and $AgNO_3$ staining methods. To run a high-resolution 2D gel electrophoresis, isoelectric focusing (IEF) was first performed as described earlier (Farhadi et al. 2011). The second dimension separation was performed using a 12.5% gel according to Laemmli. The gel was stained by silver nitrate.

Assay of CAT and POX activities

CAT activity measurements were performed in PBS (0.05 M, pH 7.0) containing H_2O_2 (0.66 mM) and 100 µL of the crude enzyme extract. The progress of the reaction was monitored through the depletion of H_2O_2 at 240 nm (Beers and Sizer 1952). A standard curve obtained for the commercial CAT (Fig. S1, supplementary document) was used to calculate the results in term of mg of CAT per gram of dry biomass.

Three spectrophotometric assay methods were used for various kinetics purposes in this study. POX activity assays in the presence of phenol (0.215 µM), 4AAP (0.003 mM), and H_2O_2 (0.66 mM) followed at 516 nm and the extinction coefficient (ε_{516}= 6500 cm^{-1} M^{-1}) of quinone-imine product was used for calculation purposes (Mohammadnejad et al. 2020; Vojinović et al. 2007). POX activity measurements in the presence of guaiacol (20 mM) and H_2O_2 (0.66 mM) was followed at 470 nm and the calculations were done by using the extinction coefficient (ε_{470}= 26600 cm^{-1} M^{-1}) of the chromophoric product (Farhadi et al. 2011). Routine assays were carried out in a conventional quartz spectrophotometry cell in a total volume of 3 mL in the desired buffer solution at 20 °C.

ObPOX activity was also studied by using GASA as the organic electron-donor. These reactions were carried out in Tris-base buffer (0.05 M, pH 7.0) containing the desired amounts of GASA (ε = 9654 cm^{-1} M^{-1}) and H_2O_2 by using pure ObPOX (49 nM). The progress of each reaction was followed spectrophotometrically by monitoring the absorbance decrease at 460 nm (Mohammadnejad et al. 2020).

Optimal pH, Temperature, and stability profiles of ObPOX

The guaiacol-based assay method was used for the determination of the optimal pH of activity. These experiments were carried out in two different buffer systems [PBS (0.05 M) and Tris-base (0.05 M)] over a pH range of 3.5 to 9.5 in the presence of a constant amount of ObPOX (49 nM) at 20 °C. The pH stability of ObPOX was examined after incubation of the enzyme in Tris-buffer solution (0.05 M) with the desired pH for half-an-hour.

To determine the optimal temperature of ObPOX activity, the guaiacol-based assays in Tris-base buffer (0.05 M, pH 7.5) over a temperature range of 15 to 100 °C were repeated by employing purified ObPOX (49 nM). Similar experiments were conducted after incubation of the enzyme solution at the desired temperature for half-an-hour to examine thermal stability of ObPOX.

ObPOX inhibition, activation and inactivation

The impact of the selected effectors, including Ca^{2+}, Mn^{2+}, NaN_3, Na_2EDTA, ascorbic acid, cysteine, and glutathione, on the activity of ObPOX in the presence of guaiacol was investigated after 15 min (T_0) and 1 h (T_1) incubation of the enzyme with the desired concentration of the effector at pH 7.5 and 20 °C. The results were interpreted in terms of activation and inhibition.

Inactivation of ObPOX by its co-substrate, H_2O_2 (5.0 - 40 mM), was investigated in the presence of GASA (10 µM), as the organic substrate during one min reaction time (T_0) and after incubation of the enzyme (49 nM) with the selected concentration of hydrogen peroxide for 30 min (T_1).

Velocity Curves

Velocity curves of the ObPOX activity were obtained at 20 °C by using constant amounts of H_2O_2 (0.26 mM) and the enzyme (49 nM) in Tris-base buffer (0.05 M, pH 7.5) containing different concentrations of i) guaiacol (5.0 - 85 mM), and ii) GASA (4.0-100 µM). The velocity curve of ObPOX for H_2O_2 (0.03-2.12 mM) was obtained by using a constant concentration of guaiacol (5.0 mM) in the same buffer and temperature. All the presented data are the average of, at least, three repeated experiments. Enzymatic Kinetics constants (K_m, k_{cat}, k_{cat}/K_m) for the substrates were calculated from the corresponding Lineweaver-Burk plots of the data and the results were double checked by Eadie–Hofstee method.

Determination of blood glucose concentration using ObPOX

Blood samples were obtained from the volunteers under fasting conditions in the laboratory of Taban Interdisciplinary Diabetes Clinic (https://www.tabanclinic.com). Sample preparation, glucose determination of the samples, and statistical analyses were carried out according to previously reported procedures (Mohammadnejad et al. 2020), using purified ObPOX and HRP as the control. All the sample preparations were carried out under the guidelines of Bioethics Committee of National institute of Genetic Engineering and Biotechnology of Iran (Approval number: IR.NIGEB.EC.1398.6.24 B).

Results And Discussion

Biomass production

The seeds of basil germinated in less than 4 days and the excised explants of the young basil plant were subjected to callus induction, which occurred in less than 3 weeks with 89% of frequency, Fig. 1A, under the applied conditions. The growth curve of the callus, Fig. 1B, reveals that the linear proliferation of the cells happened between day 7 and 28 with a growth rate of 0.126 g day $^{-1}$ (5.04 g L^{-1} per day). This resulted in about 18 and 11-fold growth of the callus (wet and dry weights, respectively) during the 35-day subculture (Fig. 1B and 1C).

The biomass graph of the proliferated cells, Fig. 1C, found a correlation coefficient of 0.98 with the growth curve. However, the highest biomass accumulation (dry/wet callus weights = 6.05%) was observed on day 21 of the subculture (Fig. 1D). In contrast to Nazir et al. works (Nazir et al. 2019; Nazir et al. 2020), in this study, the basil callus was grown in darkness as the preliminary examinations showed about 13% higher POX production in darkness as compared with those proliferated under light conditions (Fig. S2 Supplementary document). In the presence of light, phenylpropanoid pathway branches from p-coumaric acid towards flavonoids (Lobiuc et al. 2017), a phenomenon that was not observed in darkness. This might relate to the observed changes in ObPOX activity. However, light had increased the biomass accumulation to 190 g L^{-1} in the solid cell culture of basil (Nazir et al. 2020), about 51% higher than that obtained biomass in this work (126.16 g L^{-1}).

Antioxidant Capacity Of The Proliferated Cells

Although phenolic compounds account for a significant part of antioxidant capacity of a plant extract, the share of other molecules especially antioxidant enzymes is also noteworthy. Methanol is a good solvent for phenolic acids and flavonoids, while most of peptides and proteins are better dissolved in water. Figure 2A and 2B, which show the correlations between the total phenolic content (TPC) and the radical scavenging activity (RSA) of the basil callus extracts, indicate that both the TPC and RSA of the methanolic extract were higher than those of the aqueous extract, 44 and 49% respectively. However, both data reveal that the biosynthesis of the phenolic compounds was increasing up to day 31. Comparing Fig. 2A and 2B discloses two important points. TPC of the methanolic extract increased only 2% between days 21 and 31 when there was 10.3% increase in TPC of the aqueous extract. Meanwhile, there were significant increases in the corresponding RSA values (21.3 and 28.1%, respectively). These data indicate that the synthetic developments of the basil cells were toward making molecules with higher antioxidant capacities.

Examination the activities of catalase (CAT) and ObPOX (two important antioxidant enzymes) during the linear growth of the basil callus, Fig. 2C, indicates that CAT has gradually left its role to ObPOX. In contrast to the disproportionation action of CAT on hydrogen peroxide (Eq. 1 (Grigoras 2017)), POX can accept various organic compounds as the electron-donor, which results in the production of a pair of organic radicals in addition to water during a POX catalytic cycle (Equations 2). This capability allows ObPOX to support both developmental phenomena and the active biosynthetic machine of the basil cells during proliferation and aging on the solid culture (Rezaie et al. 2020). Overlaying the graphs of the

ObPOX activity and the biomass growth (Fig. 1D) discloses that despite deceleration of the biomass rate, ObPOX activity remained increasing assumingly for the sake of the cellular biosynthetic developments (Fig. 2A and 2B) (GÓMEZ-VÁSQUEZ et al. 2004).

$$2H_2O_2 \xrightarrow{\text{Catalase}} 2H_2O + O_2 \qquad \textbf{Equation 1}$$

$$2RH + H_2O_2 \xrightarrow{\text{Peroxidase}} 2R^{\cdot} + 2H_2O \qquad \textbf{Equation 2}$$

Purification of ObPOX

Stepwise precipitation of the proteins of the basil callus crude extract (Fig. 3A) suggested collecting of the precipitate at 80% saturation of ammonium sulfate. Size-exclusion chromatography of the precipitate caused the removal of most of the unwanted proteins (Fig. 3B). Then, an extra chromatography of this enzyme on an anion-exchange column resulted in a sharp fraction (Fig. 3C), which produced one homogeneous band on SDS-PAGE (Fig. 3D). Table 1 presents the quantitative summary of this procedure.

Table 1
Quantitative results of the purification scheme applied for preparation of ObPOX from *O. basilicum* callus (100g).

Steps	Volume (mL)	Total activity (AU)	Protein (mg)	Specific activity[a] (AU mg^{-1})	Recovery (%)	Fold
Crude extract	200	15442	144.4	106.93	100	1
Ammonium sulfate (80%)	8	11710	38	308.16	75.83	2.88
Sephadex G-50	15	7230	11.7	617.94	61.74	5.77
DEAE-anion exchange	6	2179	1.75	1245.14	30.14	11.64

[a] Specific activity was calculated by using ε_{516} = 6500 cm^{-1} M^{-1} for the quinone-imine product and unit of activity was considered as the µmole(s) of the product per min.

Due to the inadequate information as well as the differences in the sources of the enzymes, degree of purity, assay methods, activity unit definitions, and the applied assay conditions, it is difficult to have a clear comparison between the data of Table 1 with the data of the reported plant POXs (Table 2). Yet, comparisons between some data are informative. For instance, the protein content of the crude extracts

of hairy roots of *Daucus carota* L. (carrot), *Ipomoea batatas* L. (sweet potato), and *Solanum aviculare* (kangaroo apple) was about 3 to 4 times higher than that of the crude extract of the basil callus (Tables 1 and 2) (de Araujo et al. 2004). But, their activities were, at least, one-seventh of the basil crude extract (106.93 AU mg^{-1}) regardless of the employed electron-donors. Interestingly, the callus of carrot (*D. carota*) had already been examined as a candidate source of plant POX (Xu et al. 1998). But the reported POX activity of its crude extract (54.0 AU/g of FW) is about one-third of the basil callus extract (Table 2).

Table 2
Production information of some reported plant POXs.

Source [Reported amount]	Assay method	N.P.S[a] & Total protein	Total POX (mg) Specific activity	MW & RZ	Unit definition
Daucus carota,	Gl[b], PBS (pH 6), 470 nm, ε = 26.6k M^{-1} cm^{-1}	1, 5.8 mg (Lw) [c]	NR [d], 2.1 U/mg	NR, NR	Oxidation of 1 µmol/min (de Araujo et al. 2004)
Ipomoea batatas,		1, 6.5 mg	NR, 15.1 U/mg		
Solanum aviculare [1 g hairy root]		1, 4.9 mg	NR, 7.6 U/mg		
Daucus carota [0.1 g callus of carrot]	Gl, PBS (pH 6),	1, NR	NR, 54.0 U/g of FW	NR, NR	Oxidation of 1 mol/min (Xu et al. 1998)
Phoenix dactylifera L. [50 g of date palm leaves]	Gl, PBS (pH 6), 470 nm (ε = 26.6k M^{-1} cm^{-1})	3, 381 (Bf) [e]	1.3 mg 906.2 (U/mg)	55 kD, NR	Oxidation of 1 µmol/min (Al-Senaidy and Ismael 2011)
Glycine Max. [1 g of soybean coat]	Gl, Citrate (pH 4.6) 470 nm (ε = 26.6k M^{-1} cm^{-1})	4, 4 mg (Bf)	NR, 1549.89 (U/mg)	44 kD, 0.5	µmol of Gl oxidized/min (Parsiavash et al. 2015)
Citrus medica [80 g of leaves]	Gl, PBS (pH 6) 470 nm,	3, 556.15 mg (Lw)	10.76 mg 62.08 kU/mg	32 kD, NR	Oxidation of 1 µmol/min (Mall et al. 2013)
Commiphora gileadensis [10 g of Arabian balsam peel]	Gl, Tris (pH 7)	4, 16.76 (Bf)	0.153 mg 9503.3 (U/mg)	40 kD, NR	1 unit of Abs. [f]/min (Almulaiky and Al-Harbi 2019)
Lycupersicon hirsulum [1kg tomatoes]	Gl, PBS (pH 5)	4, 40.24 mg (Bf)	0.77 mg 104.61 U/mg	42kD, 0.7	ΔAbs. /mg prot./min (Marangoni et al. 1989)

(Number of Purification Steps)[a], (Guaiacol)[b], (Lowry method)[c], (Not reported)[d], (Bradford method)[e], (Absorbance)[f], (Dimethylaminobenzoic acid)[g],, (Weight of fresh source)[h], (o-Dianisidine)[i], and ? means unclear.

Source [Reported amount]	Assay method	N.P.S[a] & Total protein	Total POX (mg) Specific activity	MW & RZ	Unit definition
Prunus domestica [700 g of plums]	Gl, McIlvaine (pH 6.5) 470 nm,	4, 1421.7 mg (Bf)	0.175 mg 2345865 (U/mg)	58 kD, NR	0.001 Abs./min/mL (Enachi et al. 2018)
Cucurbitapepo [2 kg Zucchini peel]	DMAB[g], PBS (pH 7)	5, 8040 mg (Lw)	42 mg 443 U/mg	38.8 kD, 2	oxidized DMAB µmole/min by 1 mg/mL of POX (Casella et al. 1993)
Brassica oleracea [? Broccoli stem]	Gl, Tris (pH 6), 420 nm, ε = 25.5k M^{-1} cm^{-1}	4, 47.5 mg (Bf)	0.05 mg 882 U/mg	48 kD, 0.55	Amount of oxidized Gl/min (Thongsook and Barrett 2005)
Allium sativum [?, garlic]	Gl, Acetate (pH 5), 470 nm	4, 497 mg (Bf)	0.27 mg 13,860 U/mg	36.5 kD, NR	0.1 Abs./min (Marzouki et al. 2005)
Eupatorium odoratum [?, leaves]	ABTS, Acetate (pH 5), 405 nm, ε = 36.8k M^{-1} cm^{-1}	4, 1509 mg (NR)	2.2 mg 7094 U/mg	55 kD, NR	Oxidation of 1µM/min (Rani and Abraham 2006)
Sorghum bicolor [50g of grains]	ABTS, Acetate (pH 4), 405 nm,	5, 1050 mg (Bf)	2.8 mg 1071 U/mg	38 kD, 4	1 µmol of ABTS/min (Dicko et al. 2006)
Vigna mungo [1g of Black gram husk]	oDiA[i] Acetate (pH 5.5), 460 nm (ε = 30k M^{-1} cm^{-1})	3, 22.2 mg (Bf)	0.22 mg 1215291 U/mg	36 kD, 1.9	Oxidation of 1 µmol /min (Ajila and Rao 2009)

(Number of Purification Steps)[a], (Guaiacol)[b], (Lowry method)[c], (Not reported)[d], (Bradford method)[e], (Absorbance)[f], (Dimethylaminobenzoic acid)[g],, (Weight of fresh source)[h], (o-Dianisidine)[i], and ? means unclear.

Source [Reported amount]	Assay method	N.P.S[a] & Total protein	Total POX (mg) Specific activity	MW & RZ	Unit definition
Jatropha curcas [400 g of leaves]	Gl, Citrate (pH 5), 25°C 470 nm (ε = 26.6k M^{-1} cm^{-1})	4, 2880 mg (Bf)	5.0 mg 24,800 (U/mg)	48 kD, 3.2	Oxidation of 1 µmol/min (Cai et al. 2012)
Carica papaya, [25 g of unripe papaya]	Gl, PBS (pH 7), 37°C 470 nm (ε = 6.39k M^{-1} cm^{-1})	4, 230.71 mg (Bf)	3.38 mg 68.59 (U/mg)	240 kD, NR	Making 1 mmol product/min (Pandey et al. 2012)
Euphorbia tirucalli [? g of latex]	Gl, Acetate (pH 5.5)	2, 145 mg (Bf)	4 mg 126.5 (U/mg)	38.8 kD, 1.2	change of 0.1 unit Abs./min (Shukla et al. 2016)
Cytisus multiflorus [1 g of leaves and stems]	Gl, PBS (pH 6), 25°C 470 nm, ε = 5200 $M^{-1}cm^{-1}$)	4, 34.4 mg (Bf)	0.011 mg 17962 (U/mg)	49 kD 2.5	Oxidation of 1 µmol/min (Pérez Galende et al. 2016)
Zingiber officinale [2 g ginger]	Gl, Acetate (pH 5.5) 470 nm	4, 4.82 mg (Bf)	0.25 mg 13,136 (U/mg)	42 kD, NR	1 unit of Abs./min (El-Khonezy et al. 2020)

(Number of Purification Steps)[a], (Guaiacol)[b], (Lowry method)[c], (Not reported)[d], (Bradford method)[e], (Absorbance)[f], (Dimethylaminobenzoic acid)[g],, (Weight of fresh source)[h], (o-Dianisidine)[i], and ? means unclear.

In spite of discrepancies between different works (Table 2), there are POX examples from plant sources which are comparable with the results of this work such as POX of *Phoenix dactylifera* (Date palm leaves, 2.6 mg purified enzyme per 100 g of the source with a specific activity of 906.2 AU mg^{-1}) (Al-Senaidy and Ismael 2011), and POX of *Glycine Max*. (Soybean) coat with a specific activity of 1549.89 (AU mg^{-1}) (Parsiavash et al. 2015). There are also results with exceptionally high values such as POX of *Citrus medica* leaves (13.45 mg purified enzyme per100 g of the source with a specific activity of 62080 AU mg^{-1}) (Mall et al. 2013).

It is noteworthy to mention that the yields of HRP per unit weight of radish are highly variable and depend on climatic and other factors (Walwyn et al. 2015). In view of this fact, the commercial HRP is sold with different grade of purity including low (150 AU mg^{-1}), medium (250–330 AU mg^{-1}), and high (> 330 AU mg^{-1}) based on guaiacol assay at 25°C (Walwyn et al. 2015). Comparing the specific activity of the

purified ObPOX (1245.14 AU mg^{-1}) with a commercial HRP (206.35 AU mg^{-1}), which had been assayed with the same method of this research (Farhadi et al. 2011), discloses the potential activity of ObPOX.

Physicochemical properties of ObPOX

The SDS-PAGE analysis (Fig. 3D) suggested an average MW of 40 kD for the monomer of ObPOX, which was close to the MW of many plant POXs such as of HRP (40–46 kD) (Barnard 2012), and *Commiphora gileadensis* (Arabian balsam) (40 kD) (Almulaiky and Al-Harbi 2019) POXs. Two-dimensional electrophoresis of ObPOX resulted in separation of several spots with MW ranging from 38 to 60 kD and pI between 5 to 5.5 (Fig. S3 supplementary document). Isozyme-multiplicity in Class III plant peroxidases originates from a ubiquitous multigene family of the enzyme, post-translational modifications, and the length and number of associated glycan chains (González-Rábade et al. 2012). In contrast to HRP isozymes which all show RZ values > 1, the UV-Visible spectrum of ObPOX (Fig. 4A) was quite similar to the tomato POX spectrum (RZ = 0.7 (MARANGONI et al. 1989)) suggesting an RZ value of 0.67.

Figure 4B illustrates the activity profile of ObPOX over a wide range of pH (3.0-9.5) indicating that the enzyme tolerates acidic pH(s) much better than alkaline ones. In fact, a pH change from 7.5 to 8 causes an activity loss of 40% while shifting pH from 5 to 7.5 grounds the gradual ObPOX activity increase from 70 to 100%. Examination of ObPOX activity in Tris and PBS buffers revealed the preference of the enzyme for the organic buffer over the inorganic one (Fig. 4C) and half an hour incubation of ObPOX in mediums with different pH(s) prior to the activity assays, Fig. 4B, proved instability of ObPOX at pH > 7.5, which is ascribed to the loss of the prosthetic group at alkaline mediums and alkaline denaturation (Valderrama et al. 2002). Similar optimal pH of activity and susceptibility to alkaline pH(s) have been reported for several plant POXs including those extracted from *Prunus domestica* (plums, pH 6.5) (Enachi et al. 2018), *C. gileadensis* (pH 7.0-7.5) (Almulaiky and Al-Harbi 2019), and *Arnebia euchroma* callus (7.5) (Farhadi et al. 2011).

Similar to pH sensitivity, thermal stability is an important feature that determines the applicability spectrum of an enzyme. Activity examination of ObPOX by one-minute assay in the range of 15 to 100°C disclosed activity increase of the enzyme up to 80°C, Fig. 4D. Assessing the stability of ObPOX after 30-minute incubation at the mentioned temperatures showed high thermostability of the enzyme up to 50°C while it had lost only 12% of its activity at 60°C. The thermostability plot suggests a thermal index (T_{50} = 74°C) for ObPOX. Interestingly, ObPOX could maintain about 11.1% of its activity at 90°C, Fig. 4D, while HRP, with the mean optimal of 30°C, lost about 96.4% of its activity at 70°C whit in 10 min (Mogharrab et al. 2007). Although the maximum catalytic activity of most of the studied plant POXs were in the range of 40–65°C, there were several plant POXs which passed this border. For instance, *Ficus sycomorus* pox was able to retain about 77% of its initial activity at 70°C after 30 min incubation (Abdel-Aty et al. 2018).

Kinetics of ObPOX catalytic activity

Activation And Inhibition

The adverse effects of Ca^{2+} and Mn^{2+} on the structural stability and activities of plant POXs (Class III) have been documented. The former divalent cation with an imperative impact on molecular folding acts as prosthetic group and stabilizes the POX structure through maintenance of the heme pocket structure associated with high catalytic activities and usually demonstrates stimulatory effects on plant class III peroxidases (Medda et al. 2003). However, the latter affects it presumably via disruption of the enzyme structure through binding to the thiol group (-SH) of cysteine or formation of covalent bonds with other amino acid side chains at the enzyme active site (Barnard 2012). Study the kinetics of ObPOX after incubation of this enzyme with Ca^{2+} (5mM) for 15 min and 1 hr revealed 50 and 81%, respectively, increase in the activity. In contrast, conducting similar experiments with ObPOX after incubation with Mn^{2+} (10 mM) caused 78 and 94% decrease in the enzyme activity (Table 3). Heme-POXs (Class III) are also inhibited by azide anion due to the interaction of the ion with the metal ion of a metal enzyme (Barnard 2012; Farhadi et al. 2011). The impact of N^{3-} on ObPOX as a heme-POX was also investigated in a similar way. The data of Table 3 shows that ObPOX experienced 48 and 92% loss of activity after 15 min and 1 hr incubation with N^{3-}. The inhibitory effects of some important food additives including ascorbic acid, cysteine, and glutathione on plant POXs have been demonstrated and discussed in the literature (Tao et al. 2018). Likewise, these compounds exerted inhibitory effects on the ObPOX activity (Table S1, Supplementary document). However, the most severe impact belonged to glutathione, which caused a 92% loss of ObPOX activity.

Table 3
The normalized data of ObPOX activity changes in the presence of various concentrations (mM) of $CaCl_2$, $MnCl_2$, NaN_3, and H_2O_2.

Effector	Time‡	Control†	Concentration (mM)						
			0.5	1	5	10	15	20	40
$CaCl_2$	T_0	100	-	105.58 ± 4.36	149.74 ± 4.06	128.42 ± 4.26	115.73 ± 3.8	-	-
	T_1	100	-	124.24 ± 2.89	181.31 ± 2.97	150 ± 5.067	130.80 ± 4.9	-	-
$MnCl_2$	T_0	100	-	74.69 ± 1.03	35.104 ± 2.02	22.44 ± 3.028	-	-	-
	T_1	100	-	31.43 ± 0.97	21.63 ± 1.72	6.12 ± 1.13	-	-	-
NaN_3	T_0	100	-	69.84 ± 0.91	55.64 ± 2.48	52.62 ± 3.027	-	-	-
	T_1	100	-	69.31 ± 0.67	18.6 ± 1.63	7.39 ± 0.08	-	-	-
H_2O_2	T_0	100	-	-	80.87 ± 1.02	49.03 ± 2.19	-	32.87 ± 2.66	17.63 ± 1.99
	T_1	100	-	-	81.0 ± 3.28	16.16 ± 1.73	-	0.0	0.0

‡ T_0 and T_1 are 15 and 60 minutes incubation time of ObPOX with the effector prior to the activity measurements. In the case of H_2O_2, T_0 and T_1 were one and 30 minutes, respectively.

†Activity of ObPOX in the presence of guaiacol in Tris-base buffer solution (0.01 M, pH 7.5) at 25 ± 1 ⁰C was taken as the Control (100%). To study the effect of hydrogen peroxide guaiacol was replaced by GASA.

The Choice Of Electron-donor

Kinetics studies on a POX in the presence of various electron-donors are usually conducted to shed light on the functional capacity as well as the objectives of the intended research, e.g., those which aim to elucidate the ligninolytic potential of a POX select lignin precursors for the kinetics studies, and those with environmental concerns usually use phenols, chlorophenols, etc. Consequently, these kinetics studies were directed toward GASA, a synthetic diazo substrate of HRP introduced for direct, rapid, and precise determination of blood sugar (Mohammadnejad et al. 2020). In addition, the kinetics of ObPOX was studied in the presence of guaiacol as a traditional substrate of POXs for comparative purposes (Table 4). The reported K_m values of plant POXs for guaiacol ranges from 0.036 mM (*Raphanus*

raphanistrum POX) (Jovanović et al. 2018), to 113.2 mM (*P. domestica* POX) (Enachi et al. 2018). Therefore, the K_m of ObPOX (21.5 mM) reveals moderate affinity of this enzyme for guaiacol.

Table 4
Kinetics parameters of ObPOX in Tris-base buffer (0.05 M, pH 7.5) at 20°C.

Substrate	K_m (mM)	V_{max} (μM min^{-1})	K_{cat} (s^{-1})	k_{cat}/K_m (s^{-1} M^{-1})
Guaiacol [a]	21.5	20.1	6.80	316.41
GASA[a]	0.053	10.4	3.54	66743.7
H_2O_2[b]	0.802	0.794	0.526	655.86
[a] Activity was measured using 0.26 mM H_2O_2. [b] Activity was measured using 5.0 mM guaiacol.				
All the reactions were carried out in the presence of a constant amount of ObPOX (49 nM).				

Using guaiacol as the substrate, the affinity of ObPOX for H_2O_2 was also evaluated. The outcome (K_m = 0.802 mM, Table 4) was indicative of high affinity of ObPOX for hydrogen peroxide as compared with that of HRP (K_m = 3.7 mM) (Barnard 2012), but in an overall view, ObPOX has a moderate affinity for H2O2 ifit is compared POXs of other plants such as pencil tree latex (*Euphorbia tirucalli*, K_m = 15 mM), white lead tree (*Leucaena leucocephala*, K_m = 5.6 mM), Oil palm leaf (*Elaeis oleifera*, K_m = 1.3), and papaya fruit (*Carica papaya*, K_m = 0.25 mM) (Jovanović et al. 2018).

In contrast to the moderate affinity for guaiacol, ObPOX showed an exceptionally strong affinity for GASA (K_m = 0.053 mM, Table 4). This, in turn, gave a high specificity constant (k_{cat}/K_m) to GASA (66743.7 $s^{-1}M^{-1}$), which was promising of the high sensitivity of ObPOX to this substrate in the joint-enzymatic assay of glucose. Prior to the glucose determination tests, it was necessary to optimize H_2O_2 concentration. Gradual inactivation of POX in the presence of high concentrations of H_2O_2 triggers poor reproducibility and failure of the subsequent assays (Valderrama et al. 2002). Studies have revealed that the optimal concentration of H_2O_2 is heavily reliant on the chemical nature of the reducing substrates (Jovanović et al. 2018; Shigeto and Tsutsumi 2016). Therefore, the inactivation of ObPOX by hydrogen peroxide was studied in the presence of GASA (Table 3). Consequently, H_2O_2 (5mM) causing only 20% enzyme inactivation was selected as the best concentration for these experiments.

Determination of blood glucose concentration

The joint-enzymatic assay of blood sugar is based on the oxidation of glucose by glucose oxidase that produces equimolar of D-gluconic acid and H_2O_2. Then, HRP converts hydrogen peroxide to water by the help of an electron donor (Majumdar et al. 2016). In Trinder method, which is the base of several commercial kits and clinical measurement methods, phenol is used beside 4-aminoantipyrin. Consequently, upon enzymatic oxidation of phenol, a red color (ε = 6500 cm^{-1} M^{-1}) is developed that can

be measured at 510 nm by a simple spectrophotometer (Farhadi et al. 2011; Mohammadnejad et al. 2020). Due to the high concerns about the accurate reading of blood glucose and some problems associated with the Trinder method, some other spectrophotometric methods have been developed. In the more recent one, by using GASA as the electron-donor, it was shown that blood sugar could be determined precisely in less than 20 seconds (Mohammadnejad et al. 2020). To evaluate the applicability of ObPOX in the joint-enzymatic measurement of glucose, the blood samples of 20 participants were analyzed by an authorized clinical lab and GASA method using both HRP and ObPOX (Table 2S, Supplementary document).

Figure 5A and 5B illustrate Pearson's analysis of the blood sugar determinations by HRP-GASA and ObPOX-GASA methods versus the lab results. Accordingly, there is a higher correlation between the lab and ObPOX-GASA measurements (r = 0.98) as compared with that of HRP-GASA method (r = 0.95). The independent t-test (Table 5) rejects any statistically significant difference between these results. Nonetheless, the larger regression constant of the ObPOX-GASA correlation diagram (Fig. 5B) discloses the higher precision of ObPOX-GASA method over the HRP-GASA method. This could be ascribed to the better sensitivity of ObPOX to GASA in comparison with HRP.

Table 5
Independent t-test analysis of the results of the blood glucose determination by three independent methods of Laboratory (Lab), GASA $_{(HRP)}$ and GASA $_{(ObPOX)}$.

Methods	Regression analysis		*p*-value ≤ 0.01
Lab vs GASA $_{(HRP)}$	Y = 0.9634x + 0.1851	R^2 = 0.96	N.S*
Lab vs GASA $_{(Ob.POX)}$	Y = 0.9468 + 6.7394	R^2 = 0.96	N.S
GASA $_{(HRP)}$ vs GASA $_{(Ob.POX)}$	Y = 0.9421 + 3.8757	R^2 = 0.98	N.S
* Not significant.			

Conclusion

The callus culture of *O. basilicum* seems to be reliable source for in-vitro production of both phenolic acids and peroxidase. This assumingly originates from the high antioxidant capacity of the plant. However, depending on the goals, the applied conditions for the callus proliferation differs from one another. Studying the growth of basil callus on MS medium containing 2,4-D and kinetin in darkness and the absence of any type of elicitors revealed concomitant increase in production of the phenolic compounds and peroxidase during a 35-day subculture. The produced peroxidase showed 4 times higher affinity for phenol, as compared with that of HRP, as well as an exceptionally high specificity constant for a diazo substrate introduced for accurate determination of blood sugar. The better performance of this peroxidase in the blood glucose determination in the real samples was demonstrated.

Abbreviations

POX	Peroxidase	DEAE-C	Diethylaminoethyl cellulose
HRP	Horseradish peroxidase	MS	Murashige and Skoog medium
ObPOX	*Ocimum basilicum* peroxidase	TPC	Total phenolic compounds
PMSF	Phenylmethylsulfonyl fluoride	RSA	Radical scavenging activity
4AAP	4-Aminoantipyrine	IEF	Isoelectric focusing
2,4-D	2,4-dichlorophenoxyacetic acid	CAT	Catalase
TEMED	Tetramethylethylenediamine		
GASA	4-[(4-Hydroxy-3-methoxyphenyl) azo]-benzene sulfonic acid		

Declarations

Ethical approval

The study was autonomously reviewed and approved by ethic committee of National Institute of Genetic Engineering and Biotechnology (NIGEB), with Approval number: IR. NIGEB. EC.1398.6.24 B, affiliated to Iran's ministry of Science, Research & Technology.

Supporting information

Supporting information may be found in the online version of this article.

Conflict of interest

The authors declare no conflict of interest of any kind regarding this research article.

Acknowledgments

Funding was provided by National Institute for Genetic Engineering and Biotechnology in collaboration with Paris University (Project 730).

References

Abdel-Aty AM, Hamed MB, Gad AAM, El-Hakim AE, Mohamed SA (2018) Ficus sycomorus latex: An efficient alternative Egyptian source for horseradish peroxidase in labeling with antibodies for immunodiagnostic kits. Vet World 11:1364. https://doi.org/10.14202/vetworld.2018.1364-1370.

Ajila C, Rao UP (2009) Purification and characterization of black gram (Vigna mungo) husk peroxidase. J Mol Catal B Enzym 60:36-44. https://doi.org/10.1016/j.molcatb.2009.03.014.

Al-Senaidy AM, Ismael MA (2011) Purification and characterization of membrane-bound peroxidase from date palm leaves (Phoenix dactylifera L.). Saudi J Biol Sci 18:293-298. https://doi.org/10.1016/j.sjbs.2011.04.005.

Almulaiky YQ, Al-Harbi SA (2019) A novel peroxidase from Arabian balsam (Commiphora gileadensis) stems: Its purification, characterization and immobilization on a carboxymethylcellulose/Fe3O4 magnetic hybrid material. Int J Biol Macromol 133:767-774. https://doi.org/10.1016/j.ijbiomac.2019.04.119.

Barnard A (2012) The optimization of the extraction and purification of horseradish peroxidase from horseradish roots. Stellenbosch: Stellenbosch University

Beers RF, Sizer IW (1952) A spectrophotometric method for measuring the breakdown of hydrogen peroxide by catalase. J Biol chem 195:133-140. https://doi.org/10.1016/s0021- 9258(19)50881-x.

Cai F, OuYang C, Duan P, Gao S, Xu Y, Chen F (2012) Purification and characterization of a novel thermal stable peroxidase from Jatropha curcas leaves. J Mol Catal B Enzym 77:59-66. https://doi.org/10.1016/j.molcatb.2011.12.002.

Casella L, Gullotti M, Poli S, Ferrari RP, Laurenti E, Marchesini A (1993) Purification, characterization and catalytic activity of anionic zucchini peroxidase. BioMetals 6:213-222. https://doi.org/10.1007/bf00187758.

de Araujo BS, de Oliveira JO, Machado SS, Pletsch M (2004) Comparative studies of the peroxidases from hairy roots of Daucus carota, Ipomoea batatas and Solanum aviculare. Plant Sci 167:1151-1157. https://doi.org/10.1016/j.plantsci.2004.06.015.

Dicko MH, Gruppen H, Hilhorst R, Voragen AG, van Berkel WJ (2006) Biochemical characterization of the major sorghum grain peroxidase. FEBS J 273:2293-2307. https://doi.org/10.1111/j.1742-4658.2006.05243.x.

Efferth T (2019) Biotechnology applications of plant callus cultures. Engineering 5:50-59. https://doi.org/10.1016/j.eng.2018.11.006.

El-Khonezy MI, Abd-Elaziz AM, Dondeti MF, Fahmy AS, Mohamed SA (2020) Purification and characterization of cationic peroxidase from ginger (Zingiber officinale). Bull Natl Res Cent 44:11. https://doi.org/10.1186/s42269-019-0264-x.

Enachi E et al. (2018) Extraction, purification and processing stability of peroxidase from plums (Prunus domestica). Int J Food Prop 21:2744-2757. https://doi.org/10.1080/10942912.2018.1560311.

Farhadi S, Haghbeen K, Marefatjo MJ, Hoor MG, Zahiri HS, Rahimi K (2011) Anionic peroxidase production by Arnebia euchroma callus. Biotechnol Appl Biochem 58:456-463. https://doi.org/10.1002/bab.42.

Fehér A (2019) Callus, dedifferentiation, totipotency, somatic embryogenesis: what these terms mean in the era of molecular plant biology? Front Plant Sci 10:536. https://doi.org/10.3389/fpls.2019.00536.

GÓMEZ-VÁSQUEZ R, Day R, Buschmann H, Randles S, Beeching JR, Cooper RM (2004) Phenylpropanoids, phenylalanine ammonia lyase and peroxidases in elicitor-challenged cassava (Manihot esculenta) suspension cells and leaves. Ann Bot 94:87-97. https://doi.org/10.1093/aob/mch107.

González-Rábade N, del Carmen Oliver-Salvador M, Salgado-Manjarrez E, Badillo-Corona JA (2012) In vitro production of plant peroxidases—a review Appl Biochem Biotechnol 166:1644-1660. https://doi.org/10.1007/s12010-012-9558-2.

Grigoras AG (2017) Catalase immobilization—A review. Biochem Eng J 117:1-20. https://doi.org/10.1016/j.bej.2016.10.021.

Haghbeen K, Tan EW (1998) Facile synthesis of catechol azo dyes. J Org Chem 63:4503-4505. https://doi.org/10.1021/jo972151z.

Haida Z, Syahida A, Ariff SM, Maziah M, Hakiman M (2019) Factors Affecting Cell Biomass and Flavonoid Production of Ficus deltoidea var. kunstleri in Cell Suspension Culture System. Sci Rep 9:1-8. https://doi.org/10.1038/s41598-019-46042-w.

Jovanović SV, Kukavica B, Vidović M, Morina F, Menckhoff L (2018) Class III peroxidases: functions, localization and redox regulation of isoenzymes. In: Antioxidants and Antioxidant Enzymes in Higher Plants. Springer, pp 269-300

Khosravi E, Mousavi A, Farhadpour M, Ghashghaie J, Ghanati F, Haghbeen K (2019) Pyrrolizidine alkaloids-free extract from the cell culture of Lithospermum officinale with high antioxidant capacity. Appl Biochem Biotechnol 187:744-752. https://doi.org/10.1007/s12010-018-2830-3.

Kruger NJ (2009) The Bradford method for protein quantitation. In: The protein protocols handbook. Springer, pp 17-24

Laemmli UK (1970) Cleavage of structural proteins during the assembly of the head of bacteriophage T4. Nature 227:680-685. https://doi.org/10.1038/227680a0.

Lobiuc A, Vasilache V, Oroian M, Stoleru T, Burducea M, Pintilie O, Zamfirache M-M (2017) Blue and red LED illumination improves growth and bioactive compounds contents in acyanic and cyanic Ocimum basilicum L. Microgreens. Molecules 22:2111. https://doi.org/10.3390/molecules22122111.

Majumdar P, Khan AY, Bandyopadhyaya R (2016) Diffusion, adsorption and reaction of glucose in glucose oxidase enzyme immobilized mesoporous silica (SBA-15) particles: Experiments and modeling. Biochem Eng J 105:489-496. https://doi.org/10.1016/j.bej.2015.10.011.

Mall R, Naik G, Mina U, Mishra SK (2013) Purification and characterization of a thermostable soluble peroxidase from Citrus medica leaf. Prep Biochem Biotechnol 43:137-151. https://doi.org/10.1080/10826068.2012.711793.

MARANGONI AG, BROWN ED, STANLEY DW, YADA RY (1989) Tomato peroxidase: rapid isolation and partial characterization. J Food Sci 54:1269-1271. https://doi.org/10.1111/j.1365-2621.1989.tb05971.x.

Market Reports World. Horseradish Peroxidase (HRP) Market Size, Share 2020 Analysis, Revenue, Price, Market Share, Growth Rate, Forecast by 2024| Says Market Reports World. (2020).

Marzouki SM, Limam F, Smaali MI, Ulber R, Marzouki MN (2005) A new thermostable peroxidase from garlic Allium sativum. Appl Biochem Biotechnol 127:201-214. https://doi.org/10.1385/abab:127:3:201.

Medda R et al. (2003) Critical role of Ca2+ ions in the reaction mechanism of Euphorbia characias peroxidase. Biochemistry 42:8909-8918. https://doi.org/10.1021/bi034609z.

Mogharrab N, Ghourchian H, Amininasab M (2007) Structural stabilization and functional improvement of horseradish peroxidase upon modification of accessible lysines: experiments and simulation. Biophys J 92:1192-1203. https://doi.org/10.1529/biophysj.106.092858.

Mohammadnejad P, Asl SS, Aminzadeh S, Haghbeen K (2020) A new sensitive spectrophotometric method for determination of saliva and blood glucose. Spectrochim Acta A Mol Biomol 420 Spectrosc 229:117897. https://doi.org/10.1016/j.saa.2019.117897.

Nazir M et al. (2019) Differential production of phenylpropanoid metabolites in callus cultures of Ocimum basilicum L. with distinct in vitro antioxidant activities and in vivo protective effects against UV stress. J Agric Food Chem 67:1847-1859. https://doi.org/10.1021/acs.jafc.8b05647.

Nazir S, Jan H, Tungmunnithum D, Drouet S, Zia M, Hano C, Abbasi BH (2020) Callus Culture of Thai Basil Is an Effective Biological System for the Production of Antioxidants. Molecules 25:4859. https://doi.org/10.3390/molecules25204859.

Ochoa-Villarreal M, Howat S, Hong S, Jang MO, Jin Y-W, Lee E-K, Loake GJ (2016) Plant cell culture strategies for the production of natural products. BMB Rep 49:149. https://doi.org/10.5483/bmbrep.2016.49.3.264.

Pandey VP, Singh S, Singh R, Dwivedi UN (2012) Purification and characterization of peroxidase from papaya (Carica papaya) fruit. Appl Biochem Biotechnol 167:367-376. https://doi.org/10.1007/s12010-012-9672-1.

Parsiavash L, Saboora A, Moosavi Nejad SZ (2015) Investigating on the Stability of Peroxidase Extracted from Soybean (Glycine max var. Williams) and Effects of Na+ and K+ Ions on its Activity. J Cell Mol Res 7:94-101. https://doi.org/10.22067/jcmr.v7i2.43716.

Pérez Galende P, García de María C, Arellano JB, Roig MG, Shnyrov VL (2016) Study on extraction, purification and characterization of a novel peroxidase from white spanish broom (Cytisus Multiflorus). Int J Plant Biol Res. http://hdl.handle.net/10261/144106.

Rani D, Abraham T (2016) A potential tissue culture approach for the phytoremediation of dyes in aquaculture industry. Biochem Eng J 115:23-29. https://doi.org/10.1016/j.bej.2016.08.001.

Rani DN, Abraham TE (2006) Kinetic study of a purified anionic peroxidase isolated from Eupatorium odoratum and its novel application as time temperature indicator for food materials. J Food Eng 77:594-600. https://doi.org/10.1016/j.jfoodeng.2005.07.018.

Rezaie R, Mandoulakani BA, Fattahi M (2020) Cold stress changes antioxidant defense system, phenylpropanoid contents and expression of genes involved in their biosynthesis in Ocimum basilicum L. Sci Rep 10:1-10. https://doi.org/10.1038/s41598-020-62090-z.

Saad AI, Elshahed AM (2012) Plant tissue culture media Recent advances in plant in vitro culture:30-40

Shigeto J, Tsutsumi Y (2016) Diverse functions and reactions of class III peroxidases. New Phytol 209:1395-1402. https://doi.org/10.1111/nph.13738.

Shukla A, Gundampati RK, Jagannadham MV (2016) Biochemical and biophysical characterization of a peroxidase isolated from Euphorbia tirucalli with antifungal activity. Biocatal Biotransform 34:236-248. https://doi.org/10.1080/10242422.2016.1238463.

Tao Y-M, Wang S, Luo H-L, Yan W-W (2018) Peroxidase from jackfruit: Purification, characterization and thermal inactivation. Int J Biol Macromol 114:898-905. https://doi.org/10.1016/j.ijbiomac.2018.04.007.

Thongsook T, Barrett DM (2005) Purification and partial characterization of broccoli (Brassica oleracea Var. Italica) peroxidases. J Agric Food Chem 53:3206-3214. https://doi.org/10.1021/jf048162s.

Valderrama B, Ayala M, Vazquez-Duhalt R (2002) Suicide inactivation of peroxidases and the challenge of engineering more robust enzymes. Chem Biol 9:555-565. https://doi.org/10.1016/s1074-5521(02)00149-7.

Valdiani A et al. (2019) Bioreactor-based advances in plant tissue and cell culture: challenges and prospects. Crit Rev Biotechnol 39:20-34. https://doi.org/10.1080/07388551.2018.1489778.

Vlase L et al. (2014) Evaluation of antioxidant and antimicrobial activities and phenolic profile for Hyssopus officinalis, Ocimum basilicum and Teucrium chamaedrys. Molecules 19:5490-5507. https://doi.org/10.3390/molecules19055490.

Vojinović V, Carvalho R, Lemos F, Cabral J, Fonseca L, Ferreira B (2007) Kinetics of soluble and immobilized horseradish peroxidase-mediated oxidation of phenolic compounds BiochemEng J 35:126-135. https://doi.org/10.1016/j.bej.2007.01.006.

Walwyn DR, Huddy SM, Rybicki EP (2015) Techno-economic analysis of horseradish peroxidase production using a transient expression system in Nicotiana benthamiana. Appl Biochem 396 Biotechnol 175:841-854. https://doi.org/10.1007/s12010-014-1320-5.

Xu J, Sun Y, Su Z (1998) Enhanced peroxidase production by suspension culture of carrot compact callus aggregates. J Biotechnol 65:203-208. https://doi.org/10.1016/s0168-1656(98)00114-x.

Figures

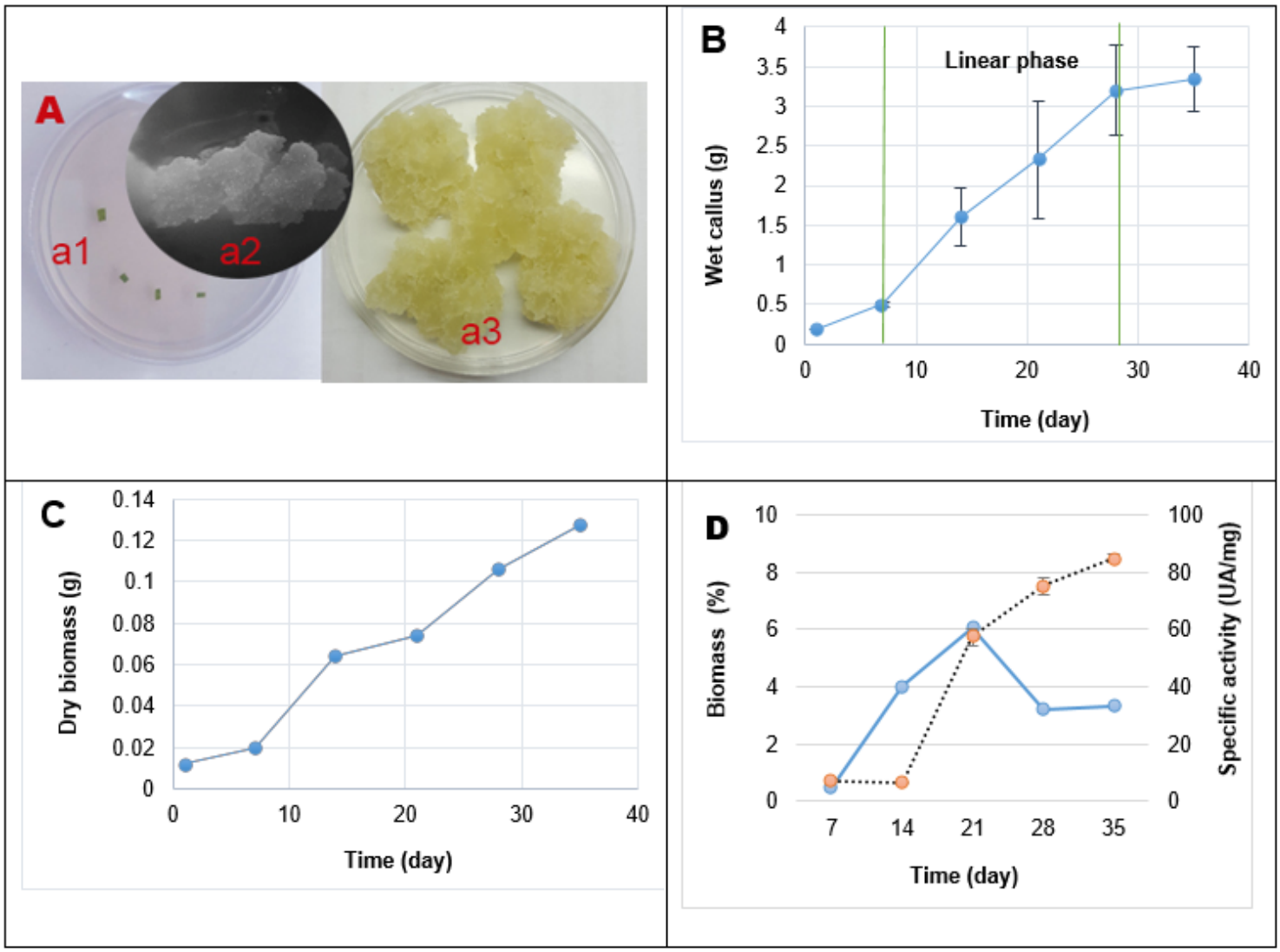

Figure 1

A) The appearance of O. basilicum leaf explants (a1), callus induction (a2), and the proliferated callus (a3) on MS medium supplemented with kinetin (10-5 M) and 2, 4-D (10-6 M) in darkness at 25±2 °C. The growth plots of B) wet basil callus and C) its dry biomass during a 35-day subculture. D) Overlaid plots of biomass (solid line) and ObPOX (dotted line) production over a period of subculture.

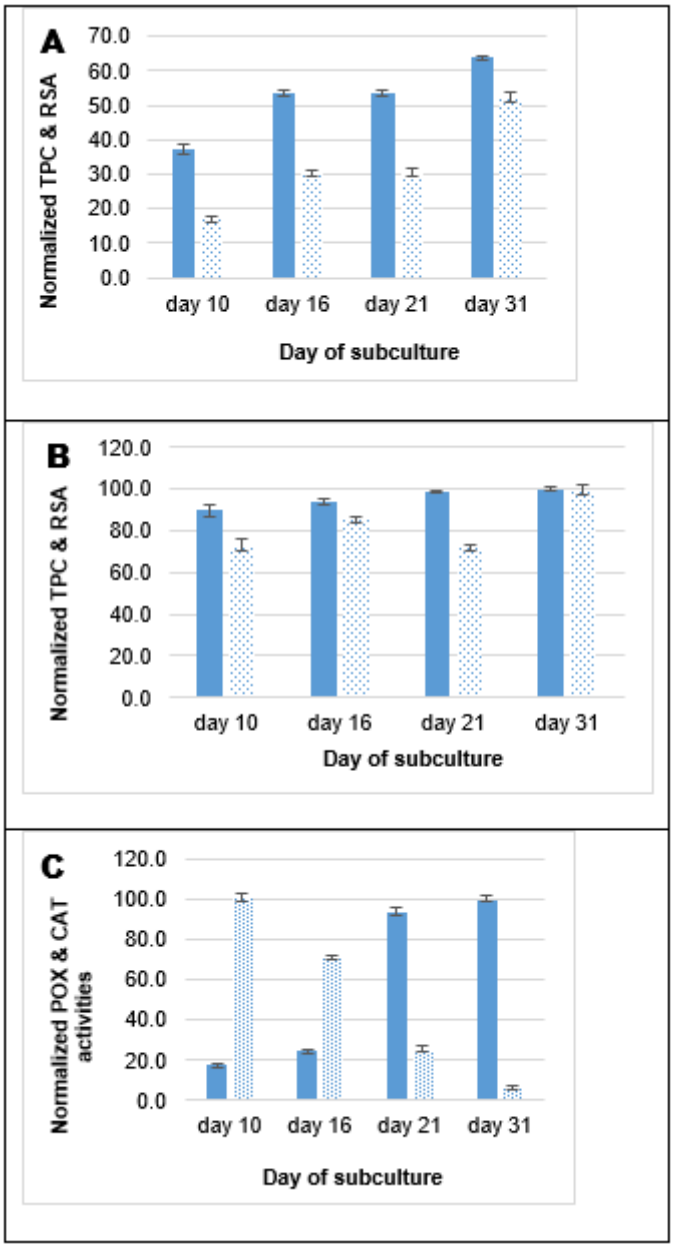

Figure 2

Normalized values of TPC (filled bars) and RSA (dotted bars) of A) aqueous (acetate buffer pH 5.5), B) methanolic extracts, as well as C) POX (filled bars), and CAT activities of the crude extract of the basil callus. Error bars show ±SD.

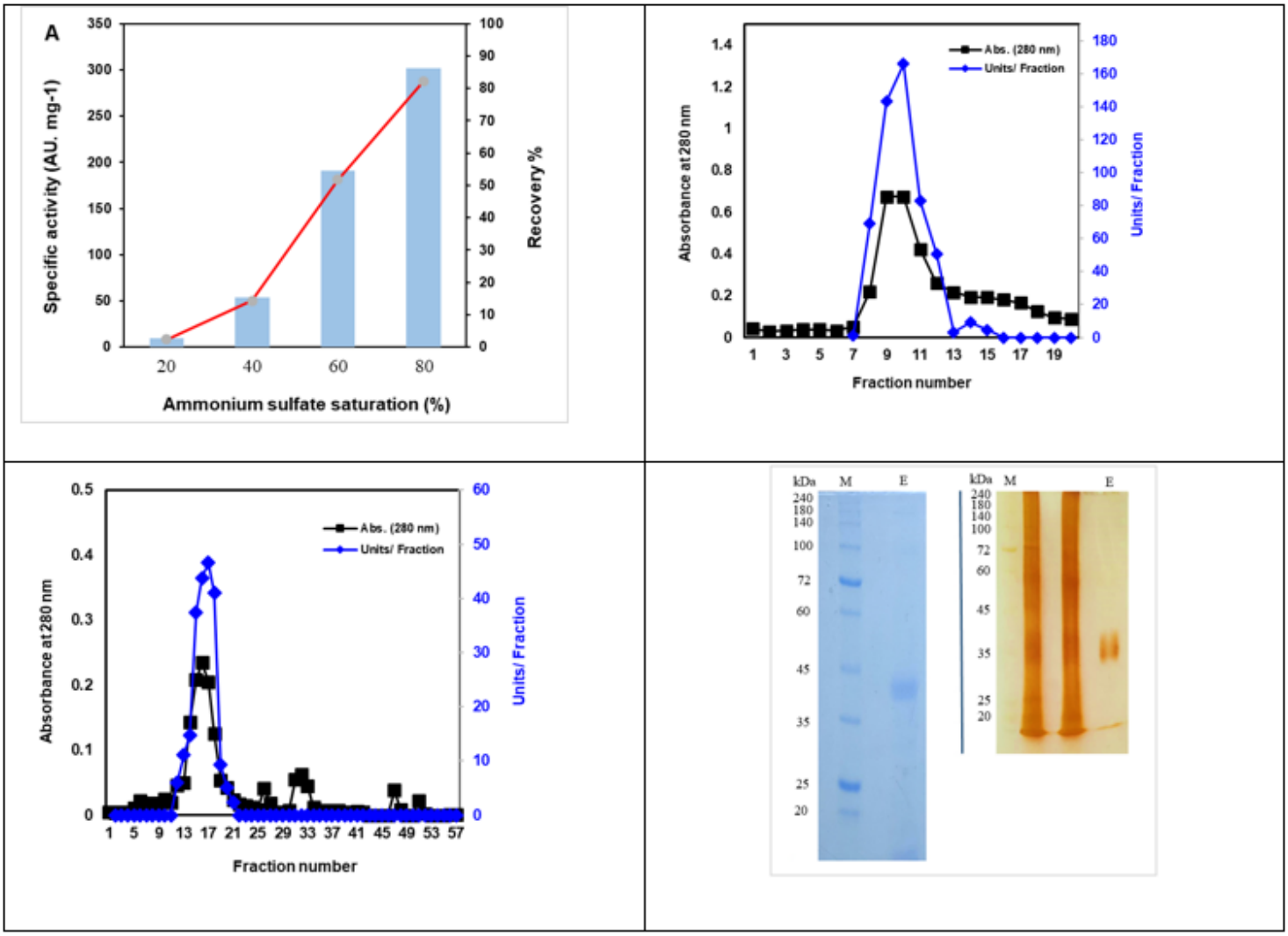

Figure 3

A) Residual activities of ObPOX in the collected precipitates at different level of saturation to ammonium sulfate. Chromatographic elution profiles of ObPOX purification on B) Sephadex G-50, and C) DEAE-C columns. E) SDS-PAGE [Coomassie blue (left) and AgNO3 (right) stain] of the purified ObPOX. M and E stand for Marker and Enzyme, respectively.

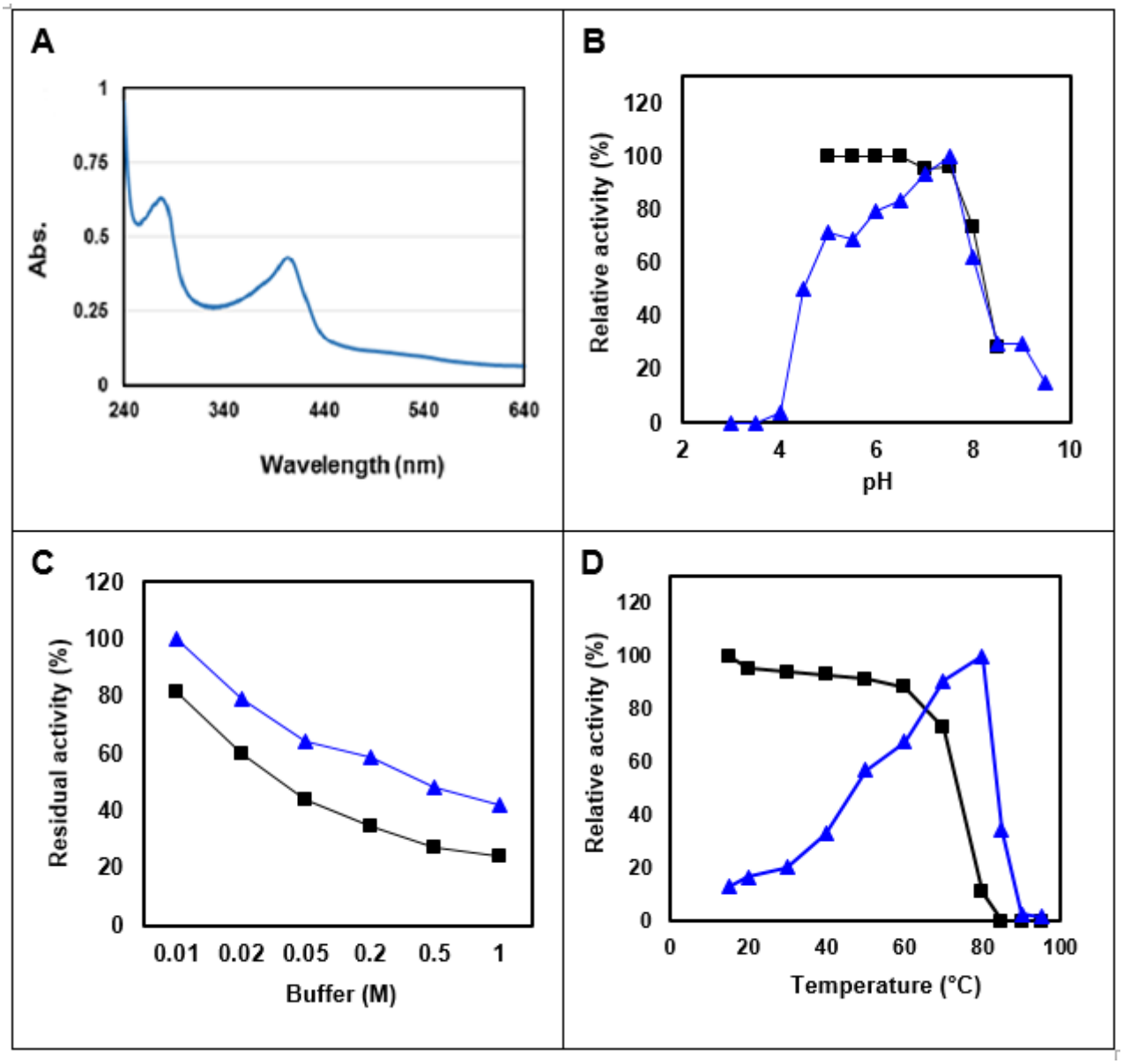

Figure 4

A) UV-Visible spectrum of ObPOX in at pH 7. B) Overlaid plots of optimal pH of activity (▲), and pH stability (■) of ObPOX at 20 ºC. C) Activity of ObPOX in Tris-base (▲) and PBS (■ buffers. D) Overlaid plots of optimal temperature of activity (▲) and thermal stability (■) of ObPOX at pH 7.

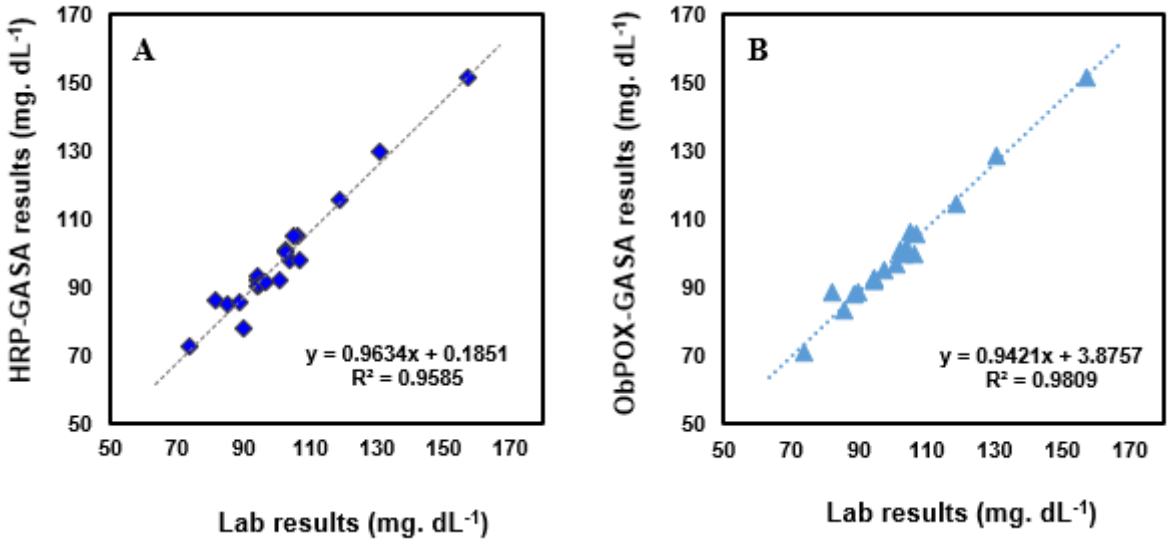

Figure 5

Pearson's correlation plots of the blood glucose determination in the blood serum samples of 20 volunteers by A) HRP-GASA, and B) ObPOX-GASA methods against the laboratory analysis results.

Supplementary Files

This is a list of supplementary files associated with this preprint. Click to download.

- Supplementarydocument.doc